Dynamics of Atmospheres and Oceans, 15 (1991) 215–240
Elsevier Science Publishers B.V., Amsterdam

The eastern Mediterranean general circulation: features, structure and variability

A.R. Robinson [1], M. Golnaraghi [1], W.G. Leslie [1], A. Artegiani [2], A. Hecht [3], E. Lazzoni [4], A. Michelato [5], E. Sansone [6], A. Theocharis [7] and Ü. Ünlüata [8]

[1] *Harvard University, Division of Applied Sciences and Department of Earth and Planetary Physics, Cambridge, MA (U.S.A.)*
[2] *Istituto di Ricerche sulla Pesca Marittima (IRSPM), CNR, Molo Mandracchio, Ancona (Italy)*
[3] *Israel Oceanographic and Limnological Research Ltd. (IOLR), Tel Shikmona, Haifa (Israel)*
[4] *Stazione Oceanografica, ISDGM, CNR, CP 316, 19100 La Spezia (Italy)*
[5] *Osservatorio Geofisico Sperimentale (OGS), CP 2011, 34016 Trieste (Italy)*
[6] *Istituto Met. e Oceanografica, IUN, Amm. Acton 38, 80133 Napoli (Italy)*
[7] *National Centre for Marine Research (NCMR), Aghios Kosmas, Hellenikon 16604, Athens (Greece)*
[8] *Institute of Marine Sciences, Middle East Technical University (IMS-METU), Erdemli, İçel (Turkey)*

(Received March 26, 1990; revised July 19, 1990; accepted July 23, 1990)

ABSTRACT

Robinson, A.R., Golnaraghi, M., Leslie, W.G., Artegiani, A., Hecht, A., Lazzoni, E., Michelato, A., Sansone, E., Theocharis, A. and Ünlüata, Ü., 1991. The eastern Mediterranean general circulation: features, structure and variability. Dyn. Atmos. Oceans, 15: 215–240.

Maps are presented for dynamic height and geostrophic flow in the upper thermocline based upon four basin-wide hydrographic surveys during 1985–1987. The data collection was coordinated, intercalibrated and pooled by the international research programme for Physical Oceanography of the Eastern Mediterranean (POEM). Objective analysis mapping was constrained to have no normal flow into the coasts. These maps reveal a new picture of the general circulation in which sub-basin-scale gyres are interconnected by jets and currents. Important variabilities occur in permanent and recurrent features but transient eddies and jets also occur. A schematic synthesis is constructed.

1. INTRODUCTION

The eastern Mediterranean Sea is isolated from the western Mediterranean Sea by the shallow and narrow Straits of Sicily. Its two major basins, the Ionian and Levantine, are shown in Fig. 1a together with the distribution of deep sea topography and the complex arrangment of coasts and islands in Fig. 1b. A knowledge of the circulation and currents of the eastern Mediterranean is of intrinsic scientific interest and necessary for regional process studies and applications. Moreover, the eastern Mediterranean, driven by a combination of water inflow and outflow, surface momentum and buoyancy

0377-0265/91/$03.50

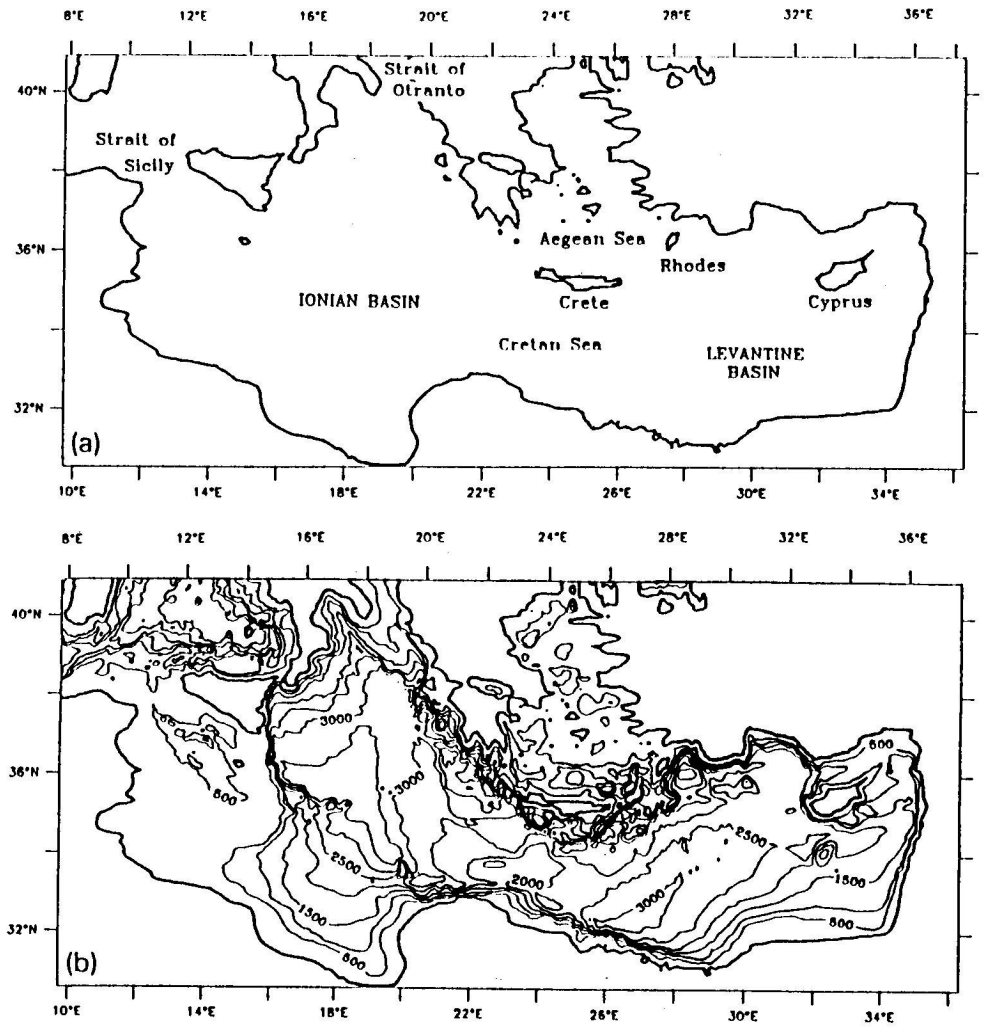

Fig. 1. (a) The eastern Mediterranean basin geography and nomenclature of the major sub-basins. (b) The bottom topography of the eastern Mediterranean Sea (contour interval is 500 m).

fluxes, forms and modifies water masses, and interacts with its overlying atmosphere. These factors together with the logistical simplification of small size make the eastern Mediterranean an ideal laboratory basin for global ocean process studies, which require a knowledge of the general circulation.

A new picture of the structure, features and variability of the eastern Mediterranean is emerging based on a new data set obtained by the international cooperative research programme for Physical Oceanography of the Eastern Mediterranean (POEM) during 1985–1987 (Malanotte-Rizzoli

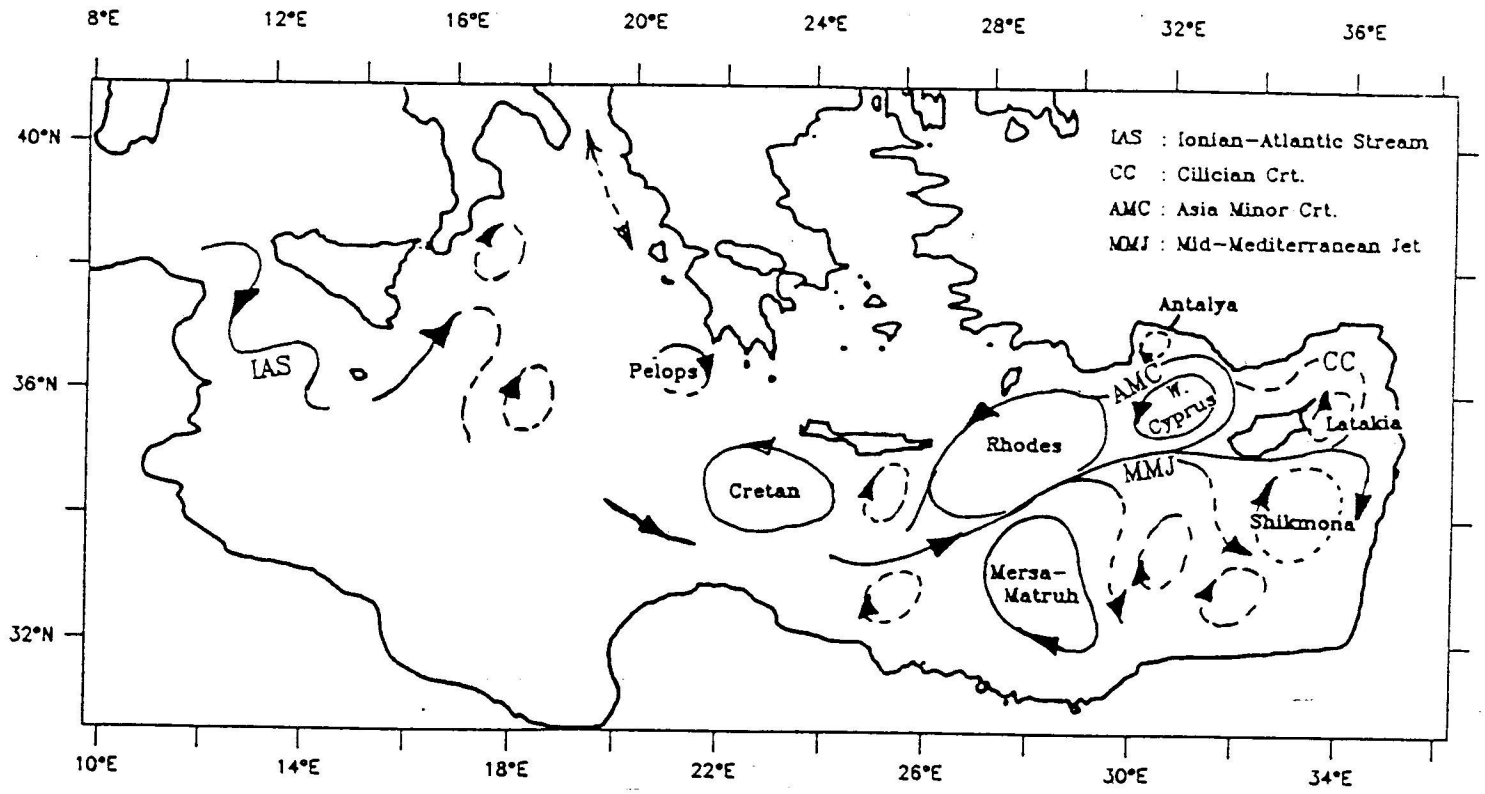

Fig. 2. Schematic general circulation. Dashed features are recurrent or transient upper thermocline.

and Robinson, 1988). Five basin-wide coordinated hydrographic surveys with nominal 1/2° sampling in latitude and longitude were carried out which provided well-resolved and nearly synoptic realizations of the circulation. The data from four surveys were intercalibrated (Michelato, 1985), pooled and shared at a workshop in Trieste in 1988. This study synthesizes the descriptive picture of the horizontal circulation pattern provided by the pooled data set. The new description differs considerably from the best previously available (Ovchinnikov, 1966; Lacombe and Tchernia, 1972; Malanotte-Rizzoli and Hecht, 1988).

The results of this paper are summarized schematically in Fig. 2. The general circulation is seen to consist of a number of sub-basin-scale gyres and eddies interconnected and interleaved by current jets and filaments. Important variabilities include:

(1) the shape, position and strength of permanent gyres;

(2) the meander pattern, bifurcation structure and strength of permanent currents;

(3) the occurrence of transient and aperiodic eddies and jets.

The results presented consist of maps of dynamic height for the upper thermocline (30/450 dbar). This depth was chosen taking into consideration both the vertical structure of the flow and the depth distribution of the hydrocasts available in the data set. The maps were constructed via objective analysis (Carter and Robinson, 1987) with correlation parameters the same as those chosen at a workshop in Modena, Italy in 1988 (Pinardi, 1988). An important consideration here concerns inhomogeneity related to the coastlines which introduce anisotropy into the analysis and constrains kinematically, the geostrophic flow. A new method of dealing with these issues, which is explained in detail in Section 2.2, is introduced and utilized. Briefly, for a strip of coast, coastal data are used to identify a coastal vertical density profile. The coastal profile is then added at intervals along the coast to the observed data set for the objective analysis. This serves both to provide the required along-coastal correlation and to impose the constraint of no normal flow into the coast.

In Section 2 we present some details of the data and the methodology. Section 3 displays and explains the maps which are discussed in Section 4.

2. DATA AND METHODOLOGY

2.1. The data

Table 1 summarizes the data from the four POEM coordinated field experiments utilized here. Included are the name of the participating institution, timetable for each cruise, the number of hydrographic stations and the depth distribution of each data set. Figure 3 a–d shows the location of the

TABLE 1

POEM data inventory as used in objective analyses

Institution	Dates	Shallow	Mid	Deep	Total
August–September 1987					
Greece–NCMR	06 Sept.–20 Oct.	2	9	101	112
Israel–IOLR	23 Aug.–10 Sept.	3	3	34	40
Italy–IRSPM	31 Aug.–18 Sept.	5	8	68	81
Italy–IUN	22 Sept.–28 Sept.	27	31	27	85
Italy–OGS	18 Aug.–13 Sept.	–	7	56	63
Turkey–IMS–METU	06 Sept.–27 Sept.	8	61	–	69
October–November 1985					
Israel–IOLR	14 Oct.–6 Nov.	–	–	80	80
Italy–ISDGM	09 Nov.–26 Nov.	9	1	7	17
Turkey–IMS-METU	31 Oct.–12 Nov.	3	8	39	50
March–April 1986					
Greece–NCMR	19 March–24 April	1	13	84	98
Israel–IOLR	06 April–31 April	–	–	64	64
Italy–IRSPM	06 May–08 May	34	–	–	34
Italy–OGS	27 March–04 April	10	11	29	50
Turkey–IMS–METU	15 April–29 April	13	9	33	55
March–April 1987					
Greece–NCMR	16 March–04 May	1	10	53	64
Italy–IUN	05 March–13 March	28	33	24	85
Turkey–IMS–METU	20 Feb.–02 March	9	10	23	42

Definitions: shallow, CTD is shallower than 450 m; mid, CTD is 450 m or deeper and shallower than 800 m; deep, CTD is 800 m or deeper.

station positions; first, for the most complete data set of August/September 1987 (AS 87), and then October/November 1985 (ON 85), March/April 1986 (MA 86) and March/April 1987 (MA 87), respectively. The symbols designate casts which are at least 450 m deep but shallower than 800 m (circles); casts which are deeper than 800 m (squares) and profile locations which are used in the objective analysis to constrain the flow along the coasts (crosses).

Data were collected by either Neil Brown or SBE-9 Seabird CTD profilers. Primary data processing and quality control was performed by the individual institutions responsible for the collection of the data based on the recommendations of the POEM Workshop on Common Procedures for Data Acquisition, Treatment and Intercalibration (Michelato, 1985). The processing procedures included pre- and post-cruise calibration of the CTD sensors. The data have been corrected according to calibration factors computed from salinity, temperature and thermometric pressure measurements acquired by rosette. The salinity was determined onboard ship or in

the shore laboratory immediately after each cruise by Autosal or equivalent salinometer. Temperature and pressure corrections have been made by individual institutions where necessary. Pinardi (1988) contains details of the processing procedures for each institution. According to such procedures, the overall estimated error in dynamic height anomaly for the depth range of interest should be < 1 dyn cm (Gregg, 1979). Final quality control of the data was performed at Harvard during the calculations of dynamic height. These calculations used the standard routines of Fofonoff and Millard (1983).

Common intercalibration stations were chosen for pairs of ships and occupied as simultaneously as possible. In order to minimize the effect of any time differences between casts the intercomparison was carried out on data deeper than 800 dbar where the eastern Mediterranean is known to be practically time-invariant. These intercalibration stations were designed to allow the merging of the data from all the different ships into a single pooled data set. The six subsets of AS 87 data set were found to require no corrections to temperature and only a single salinity offset of -0.04 psu was applied to the data from IMS–METU. For the ON 85 data set, corrections of $+0.04°$C and $+0.03$ psu have been added to the IMS–METU data. Correction factors of $+0.02°$C and $+0.03$ psu have been applied to the NCMR data and $+0.02°$C and $+0.06$ psu to the IMS–METU data for MA 86. The specific details of the intercalibration procedures for these data sets can be found in Pinardi (1988), and Özsoy et al. (1989a, b), respectively. Intercalibration is not relevant to the MA 87 isolated subregions. The data mapped prior to intercalibration corrections are seen to contain non-physical structures at the boundaries between ship domains. The structures within each ship's domain are, of course, essentially unchanged.

We initially treat the AS 87 data which provide an almost complete, nearly synoptic picture of the general circulation of the eastern Mediterranean. We then analyse the circulation patterns of the ON 85 data set, which covers the full Levantine Basin. Next follows the MA 86 data set, covering the full Levantine Basin and the northern Ionian Basin. Lastly, we analyse the MA 87 data set. These other data sets describe portions of the basin and provide regional information on seasonal and other variabilities which occur.

2.2. Coastal objective analysis

Each of the four data sets were interpolated to a regular 25-km grid and contour mapped via objective analysis schemes (Carter and Robinson, 1987). A random error of 0.1 has been assumed. We have used a time-independent, spatially isotropic correlation function given by

$$C_{(r)} = \left[1 - \left(\frac{r}{a}\right)^2\right] \exp\left[-0.5\left(\frac{r}{b}\right)^2\right]$$

TABLE 2

Domain information and OA parameters

Domain size: 2250×1150 km^2
Grid spacing: 25 km
Grid points: 103×47
Grid centre: 33.75° N, 23.00° E
OA parameters: $(a, b) = (100, 67)$; $e = 0.1$

where a, the zero-crossing correlation length scale, and b, the e-folding scale, were chosen as 100 and 67 km, respectively (Pinardi, 1988) (Table 2). Direct computation of the correlation function for the ON 85 and MA 86 data was carried out by Özsoy et al. (1989a) and for the AS 87 CTD profiles together with high-resolution XBT data for the northwest Levantine Basin at nine vertical levels by Milliff (1989). Examination of their results indicates that in the thermocline, our choice for the zero crossing is appropriate for the general circulation and sub-basin scales over our depth range, although the decorrelation scale is somewhat longer at the upper layers and decreases with depth. In any case, objectively analysed maps are insensitive to relatively small changes in these parameters owing to the overall abundance of data.

Although the data measurements are not completely synoptic, areas which have been sampled by multiple institutions were sampled as simultaneously as possible. Additionally, previous work (Hecht et al., 1988) indicates that over the time frame of the measurements, there should be little evolution of the fields.

The features and the structure of the flow as indicated by the simple isotropic objective analysis map of Fig. 4a are correct over the major part of the basin. In order to verify the mapping procedure and to eliminate the possibility of single station features, the station positions have been superimposed onto the objectively analysed fields (not shown). There are no features in the objectively analysed fields which are supported by only one observation. Aspects of the near-coastal flow, however, require a refined treatment associated with the anisotropy and kinematics of the coastal region. An example is the apparent coastal inflow and outflow along the northern Levantine boundary. The sampling scheme was designed to resolve the general circulation, and was generally not altered in the vicinity of the coastal and shelf regions. Thus, we do not attempt to map coastal and shelf phenomena. The general circulation flow is consistently constrained to have no normal flow component into the coast, which is achieved geostrophically by imposing a horizontally uniform density profile along the coast. For the most part, the basin is rimmed by a narrow shelf and steep slope, and the

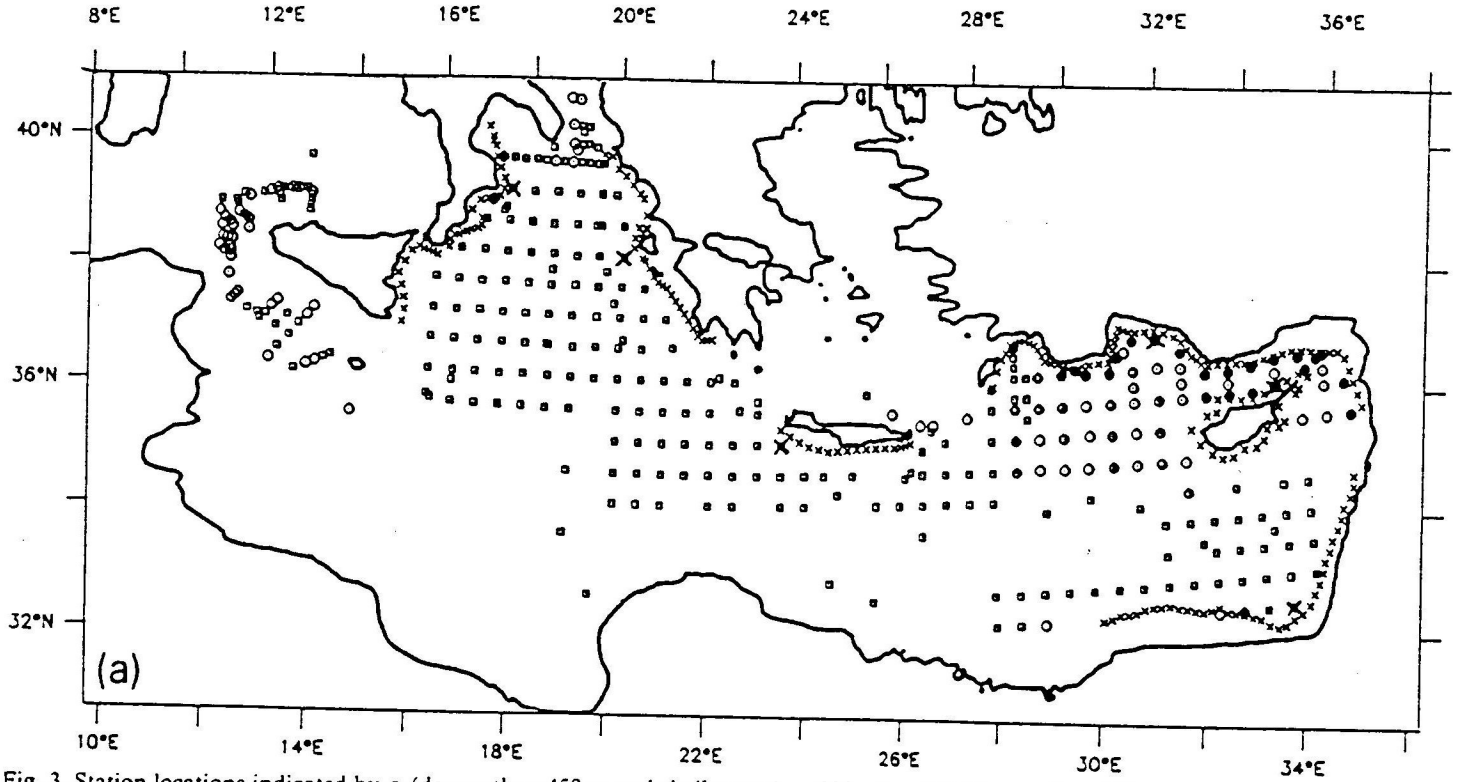

Fig. 3. Station locations indicated by ⊙ (deeper than 450 m and shallower than 800 m) and ⊡ (deeper than 800 m), near-coastal profiles used in the selection of the boundary profile ● or ■, the selected profile coastal constraint ✱ or ✱, and the positions of inserted boundary profiles ×. (a) AS 87, (b) ON 85, (c) MA 86, (d) MA 87.

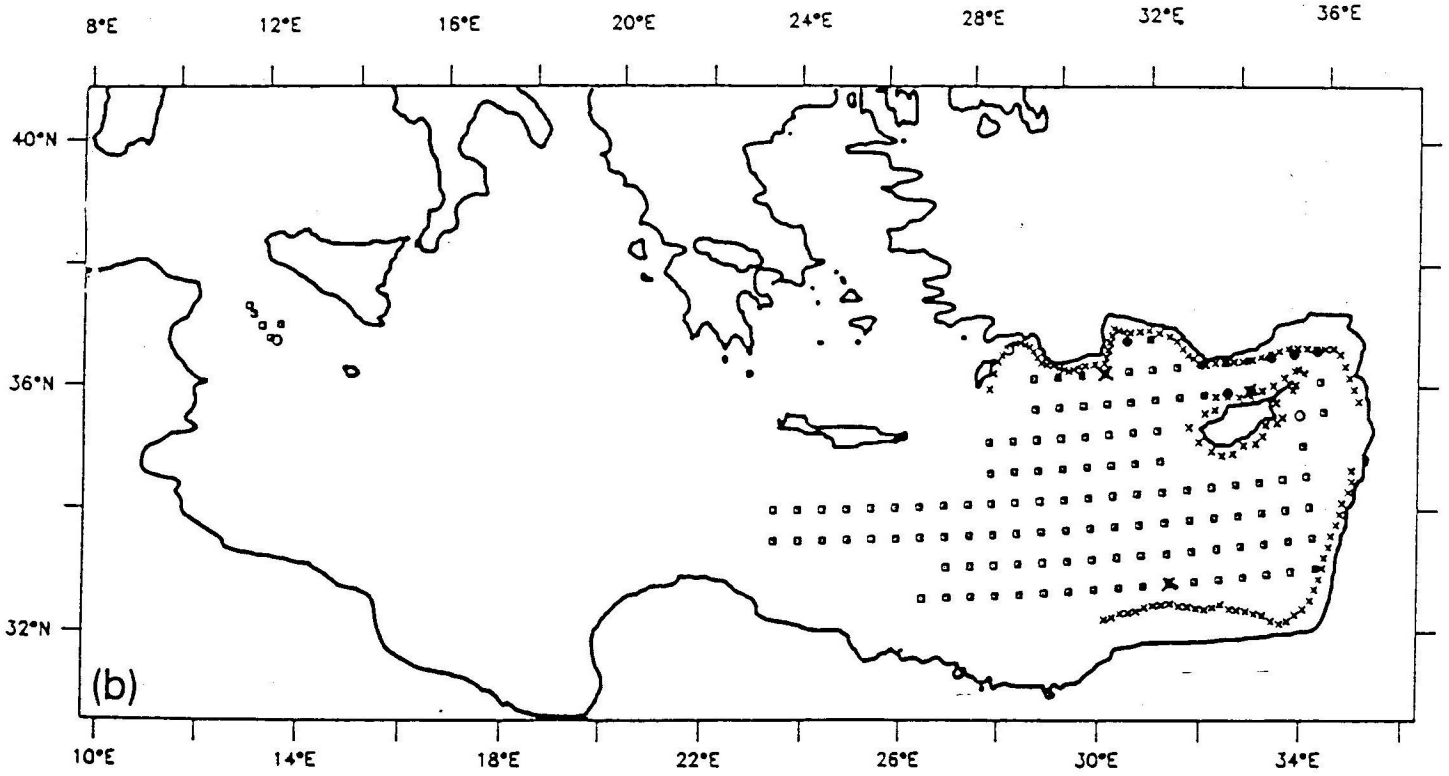

Fig. 3 (continued).

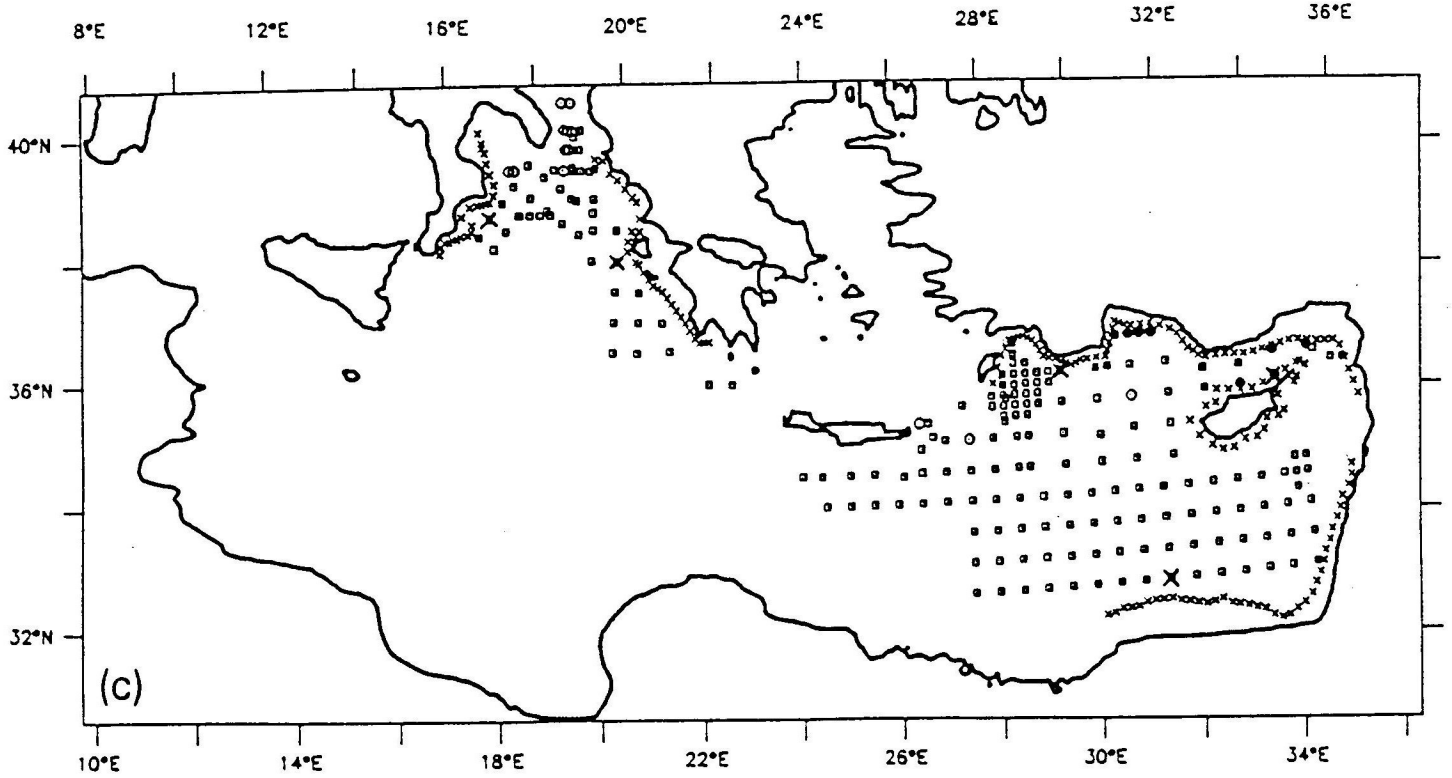

Fig. 3 (continued).

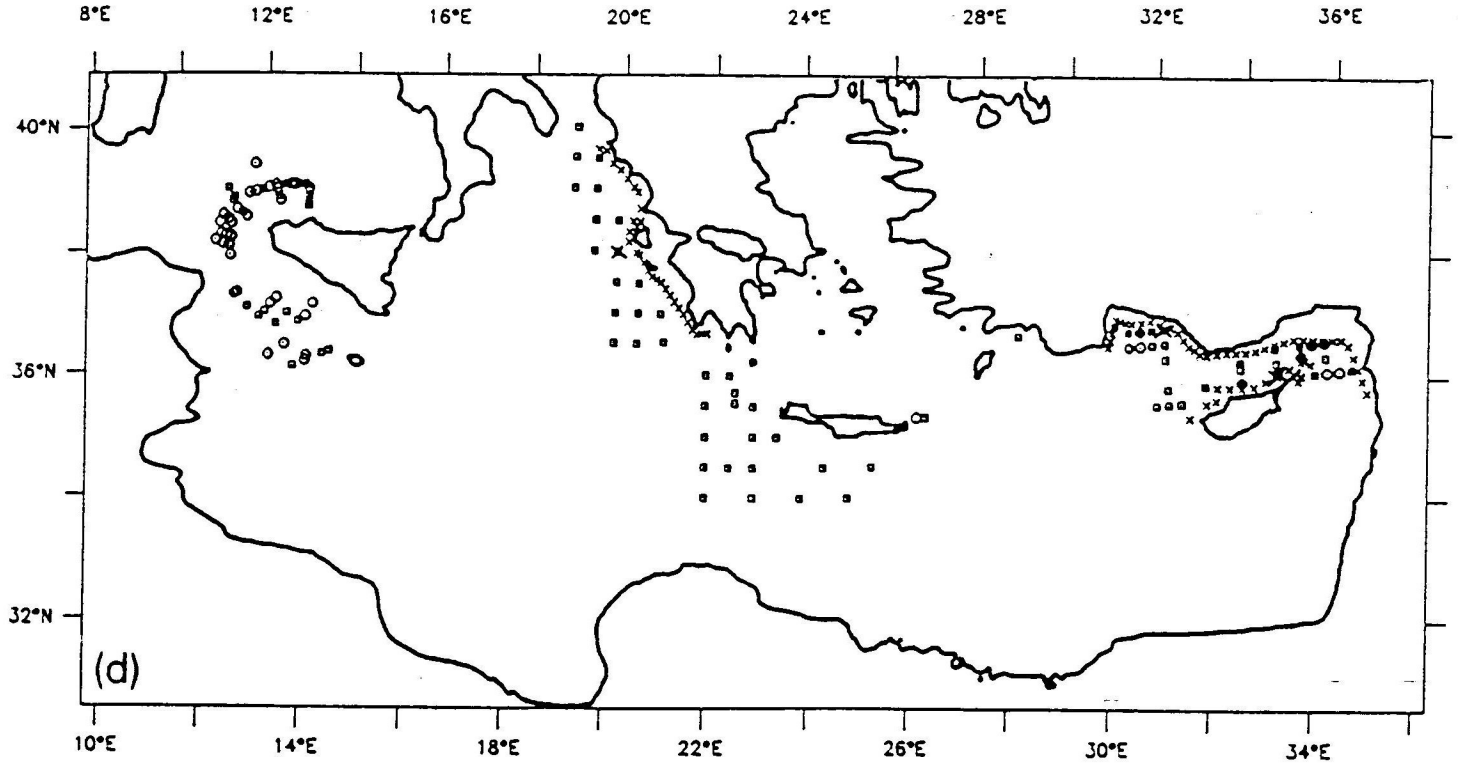

Fig. 3 (continued).

coastal kinematic constraint is imposed on the shelf-break chosen as the 600-m isobath.

In practice, the constraint is imposed by adding to the data set to be mapped, a number of boundary profiles, located along the shelf-break less than a decorrelation length apart. Although we continue to map with an isotropic correlation model, the boundary data set imposes upon the maps the required coastal anisotropy with high along-shore correlation. Segments of the coastline are characterized by a boundary profile inferred from

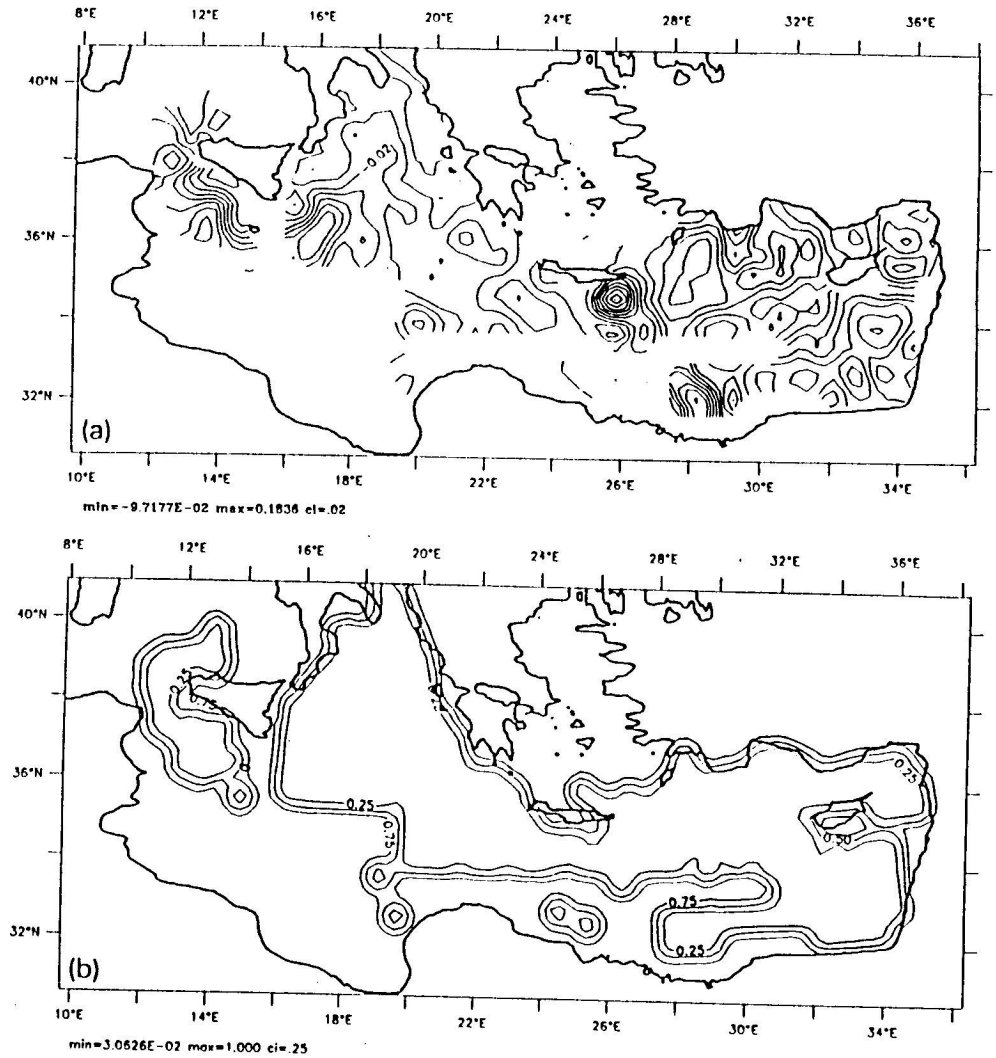

Fig. 4. (a) Dynamic height anomaly (dm) for 30/450 (dbar) for AS 87 with no coastal boundary profiles. (b) The error field.

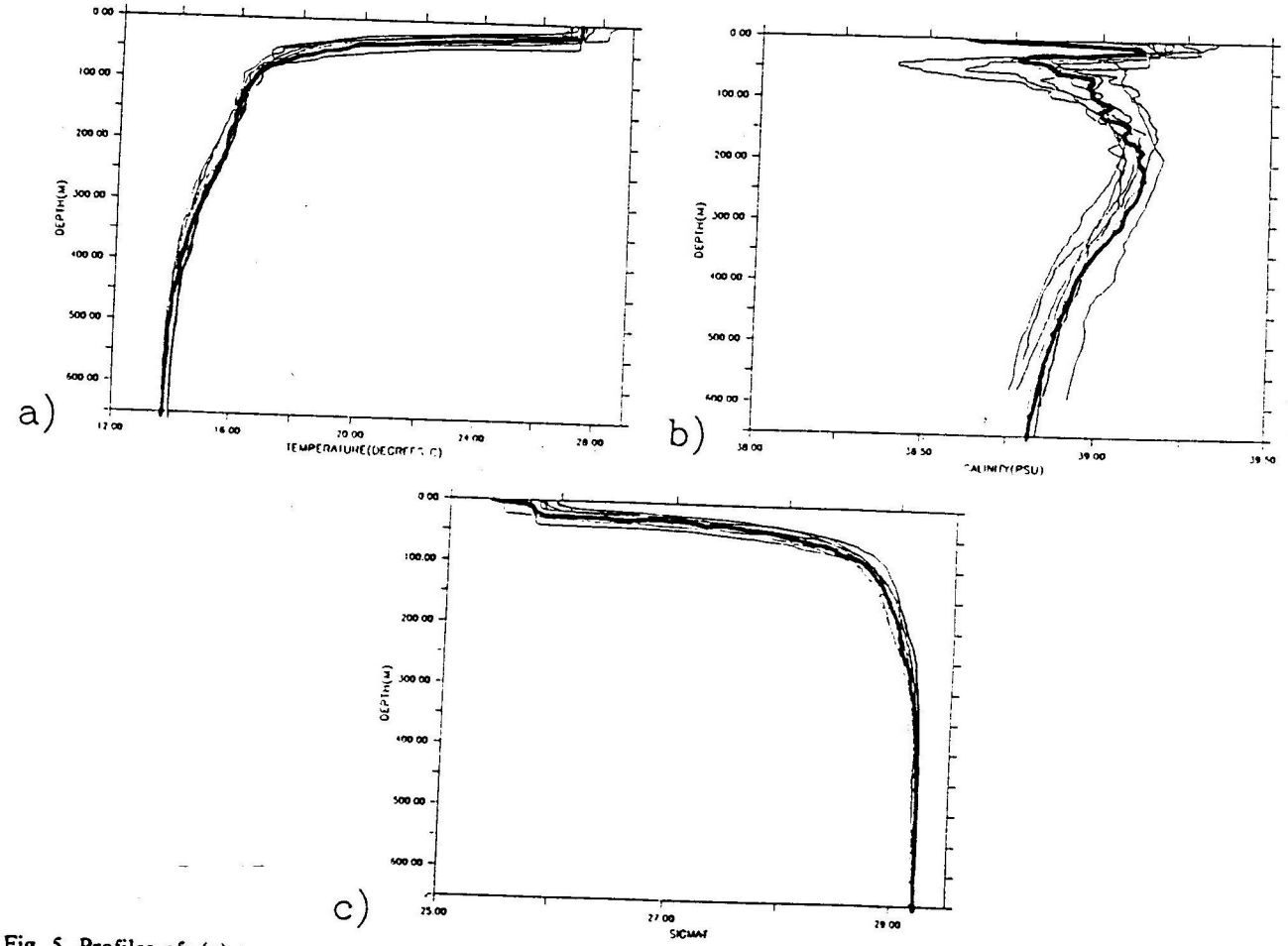

Fig. 5. Profiles of: (a) temperature; (b) salinity; (c) density (sigma-t), for the stations near the northern Levantine coastal region with the selected boundary profile identified by the darker line.

near-coastal data. The segments are selected subjectively, bounded by major straits or by gaps in near-coastal data. For the case of POEM AS 87, six boundary profiles were used for the following regions: the northwest and northeast Ionian coasts, Crete, the northern Levantine coast, Cyprus, the southern Levantine coast together with the south part of the eastern Levantine coast (Fig. 3a).

To determine the boundary profiles, the near-coastal data are examined subjectively and a representative CTD is chosen for the boundary CTD. On each of the station position maps of Fig. 3, all near-coastal data used for this purpose are indicated, and the CTD selected for the boundary profile is identified. The procedure is illustrated for the northern Levantine coastal profile in Fig. 5. Consideration in each case is given to the distance of a station to the shelf-break, the proximity of data points, data quality, etc. Tests indicate that the procedure is robust and not sensitive to the particular profile selected.

The combined observations plus boundary profile data set for POEM AS 87 has the expected error map of Fig. 6. Figure 7a can be compared with Fig. 4a; the essential patterns remain controlled by the observations. The error maps for the other data sets relate to their station positions similarly as with Figs. 3 and 6 and are not shown. The flow field of the coastal objective analysis (Fig. 7a) compared with the isotropic objective analysis (Fig. 4a) shows the same general circulation features unmodified over most of the basin but with continuous coastal currents and no flow into the coast.

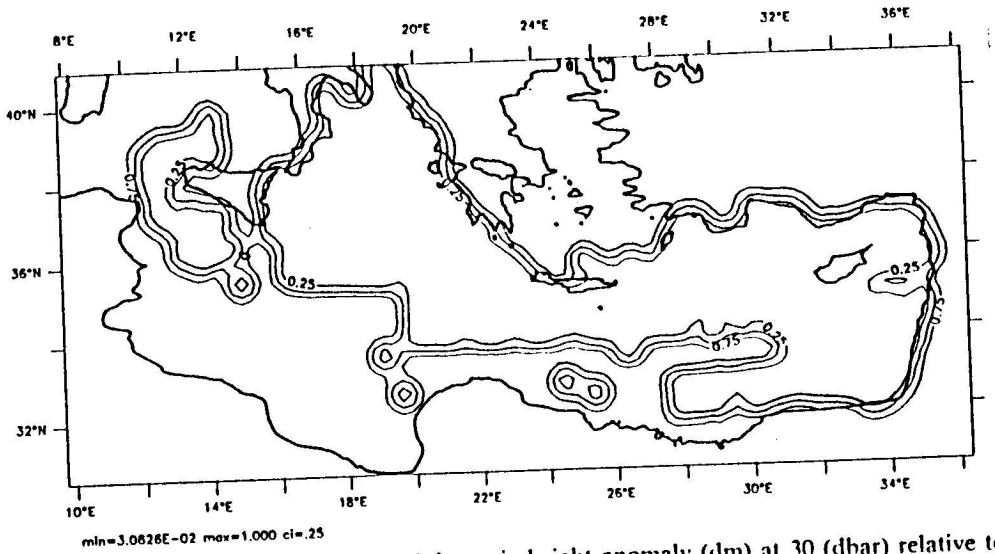

Fig. 6. The error field for the map of dynamic height anomaly (dm) at 30 (dbar) relative to 450 (dbar) for AS 87 with coastal constraint.

3. RESULTS

The results of this study are presented as a set of maps of dynamic height anomaly for the upper thermocline (30 dbar relative to 450 dbar) together with their associated relative geostrophic flow patterns (Figs. 7–10). The flow is quite complex and variable. It is useful to scan the maps in order to identify the permanent features and variabilities.

The permanent features consist of cyclonic and anticyclonic sub-basin-scale gyres fed and interconnected by jet-like currents. Variabilities of the features consist of shifts of centres, deformation and oscillation of gyre boundaries, meandering of currents, and the location and number of current branchings. Some features of the same character appear and disappear at the same place, but other features appear to be simply transient variabilities. The latter include jet segments and sub-basin-scale eddies which in this data set are all anticyclonic.

A summary of results and a descriptive synthesis of the features and circulation revealed by this analysis is contained in the schematic map of Fig. 2 and the feature table for the upper thermocline, Table 3. The classification of features into permanent, recurrent and transient is our best judgement at this time on the basis of this data set. Exceptions are that the Ionian–Atlantic stream is known to be permanent and the Shikmona eddy was classified as recurrent because observations in the region from 1979 to mid-1983 showed it to be absent (Hecht et al., 1988, fig. 16).

The most complete picture is presented by AS 87 (Fig. 7a,b). The Atlantic stream enters and meanders and loops into the Ionian. The general weak flow in the northern Ionian is anticyclonic. We believe the Ionian–Atlantic stream to be connected to the mid-Mediterranean current, which here has apparently bifurcated in the data gap. One branch flows northward above Cyprus into the Asia Minor current and the other, eastward and northward, turning to the south around the Shikmona anticyclone. The West Cyprus cyclone is strong and the Rhodes gyre is in a four-lobe pattern. Only the southern edge of the permanent strong Mersa–Matruh gyre has been mapped. The Cretan Sea cyclone and Pelops anticyclone are clearly defined. Strong eddies exist southeast of Crete, east of Cyprus and east of the Mersa–Matruh gyre. Transient eddies and jet segments occur throughout the basin.

The mid-Mediterranean current in ON 85 (Fig. 8a, b) flows relatively smoothly eastward between the borders of the Mersa–Matruh and Rhodes gyres, bifurcating to flow around a small west Cyprus cyclone and the Shikmona eddy. But now a second bifurcation leads to a flow to the north around Cyprus which feeds a meandering Cilician current which then joins the Asia Minor current. There is a general anticyclonic system in the

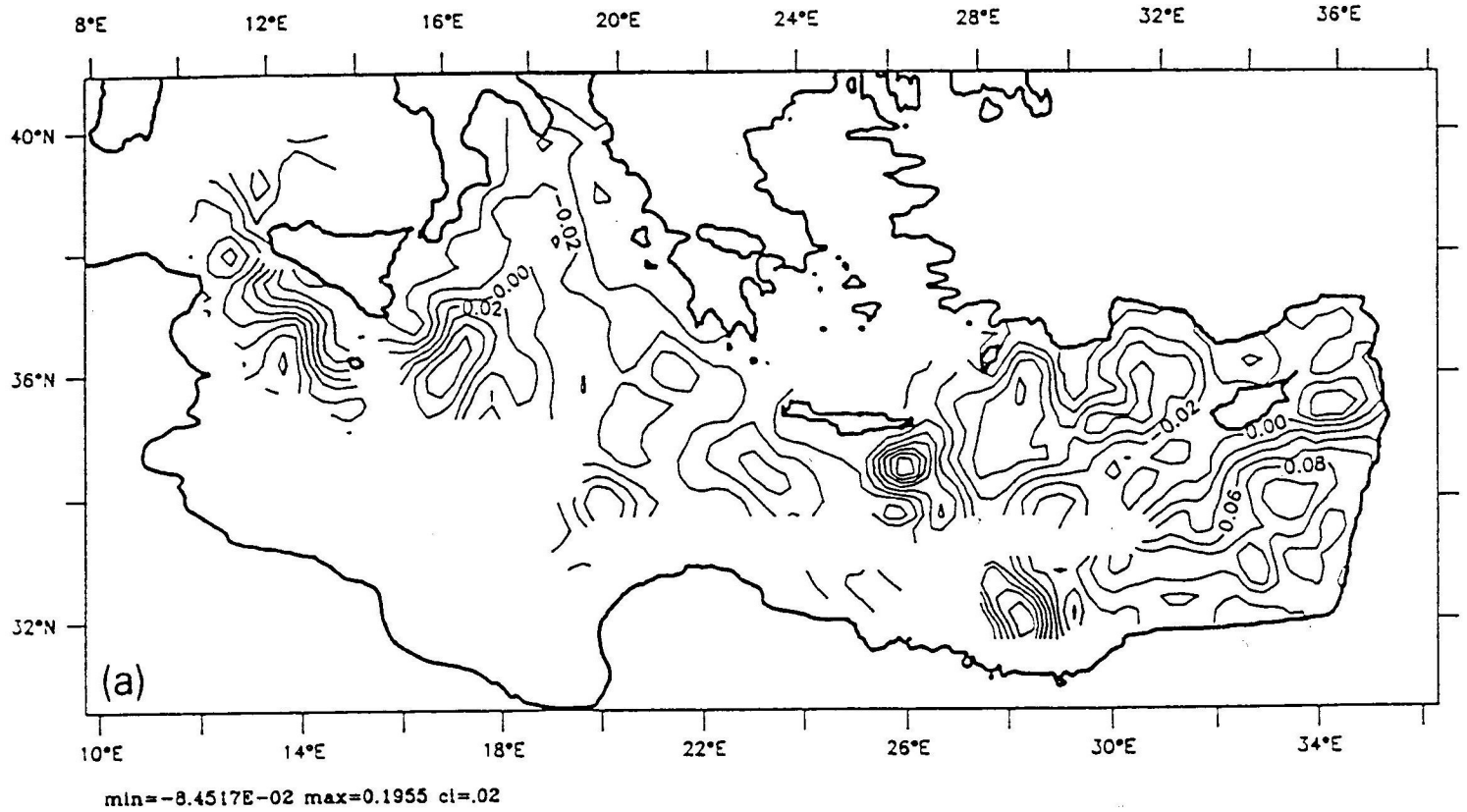

Fig. 7. (a) Dynamic height anomaly (dm), upper thermocline (30/450) with coastal constraint, AS 87. (b) Horizontal flow vectors at 30 m, AS 87.

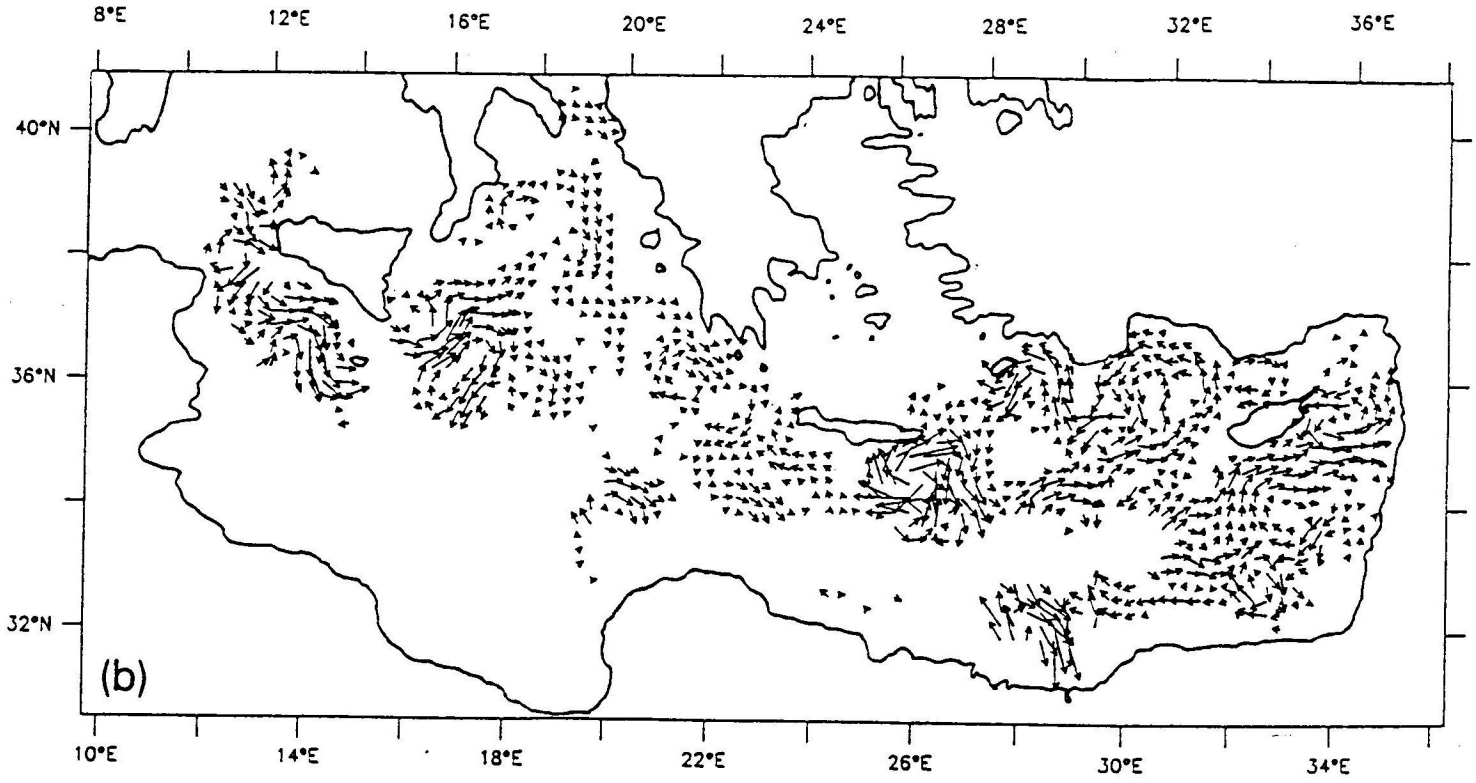

Fig. 7 (continued).

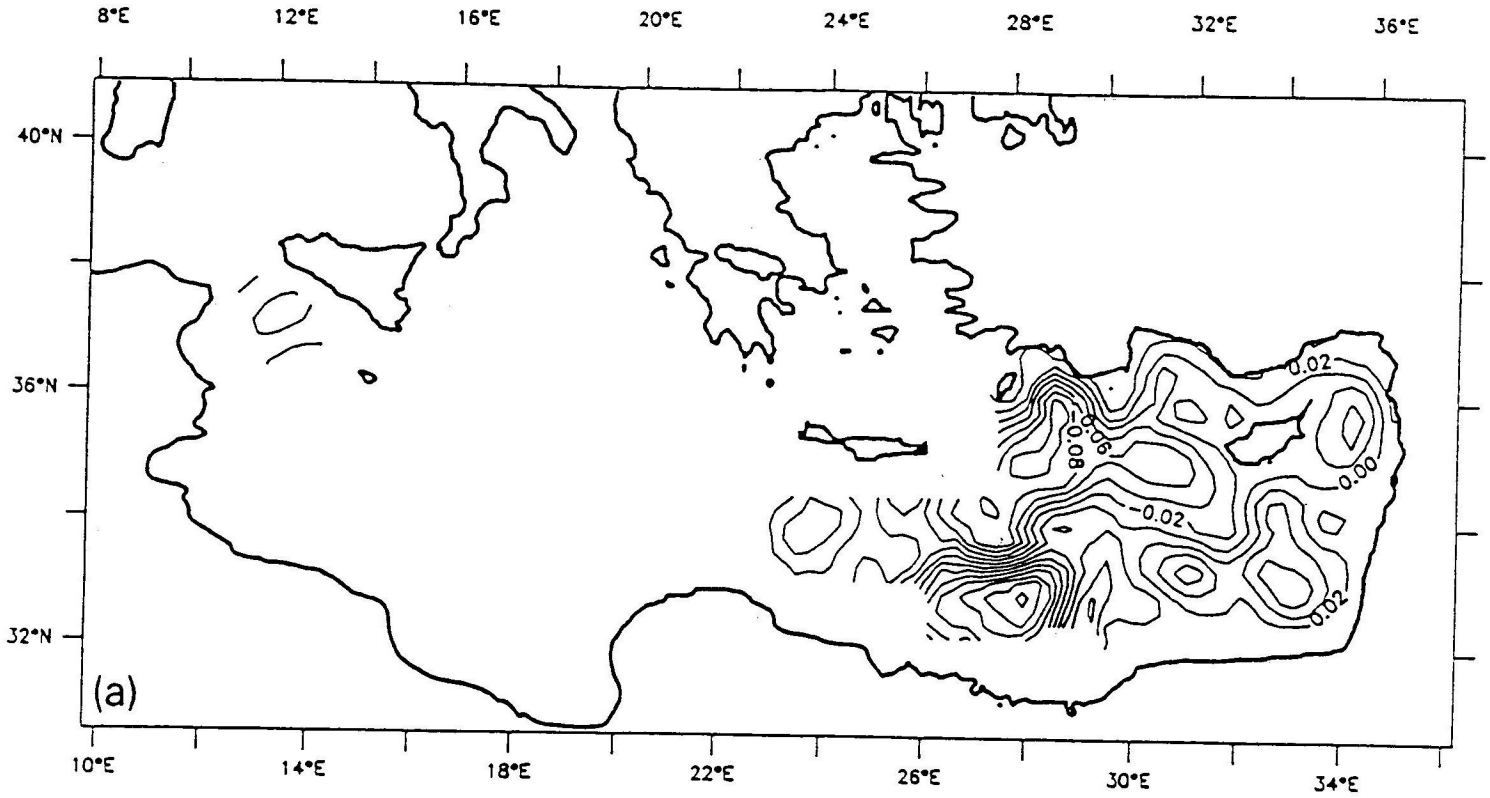

Fig. 8. As in Fig. 7 but for ON 85.

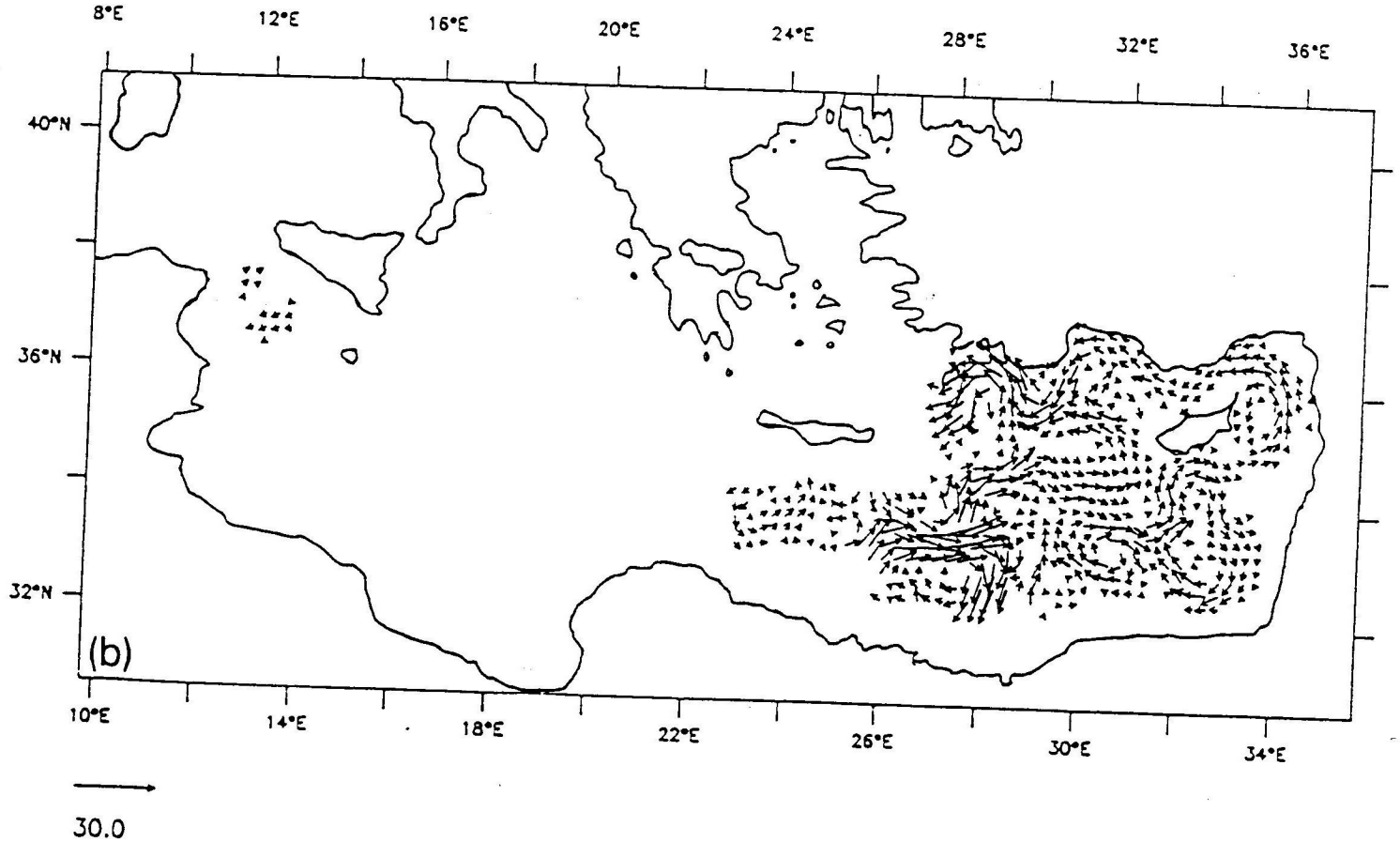

Fig. 8 (continued).

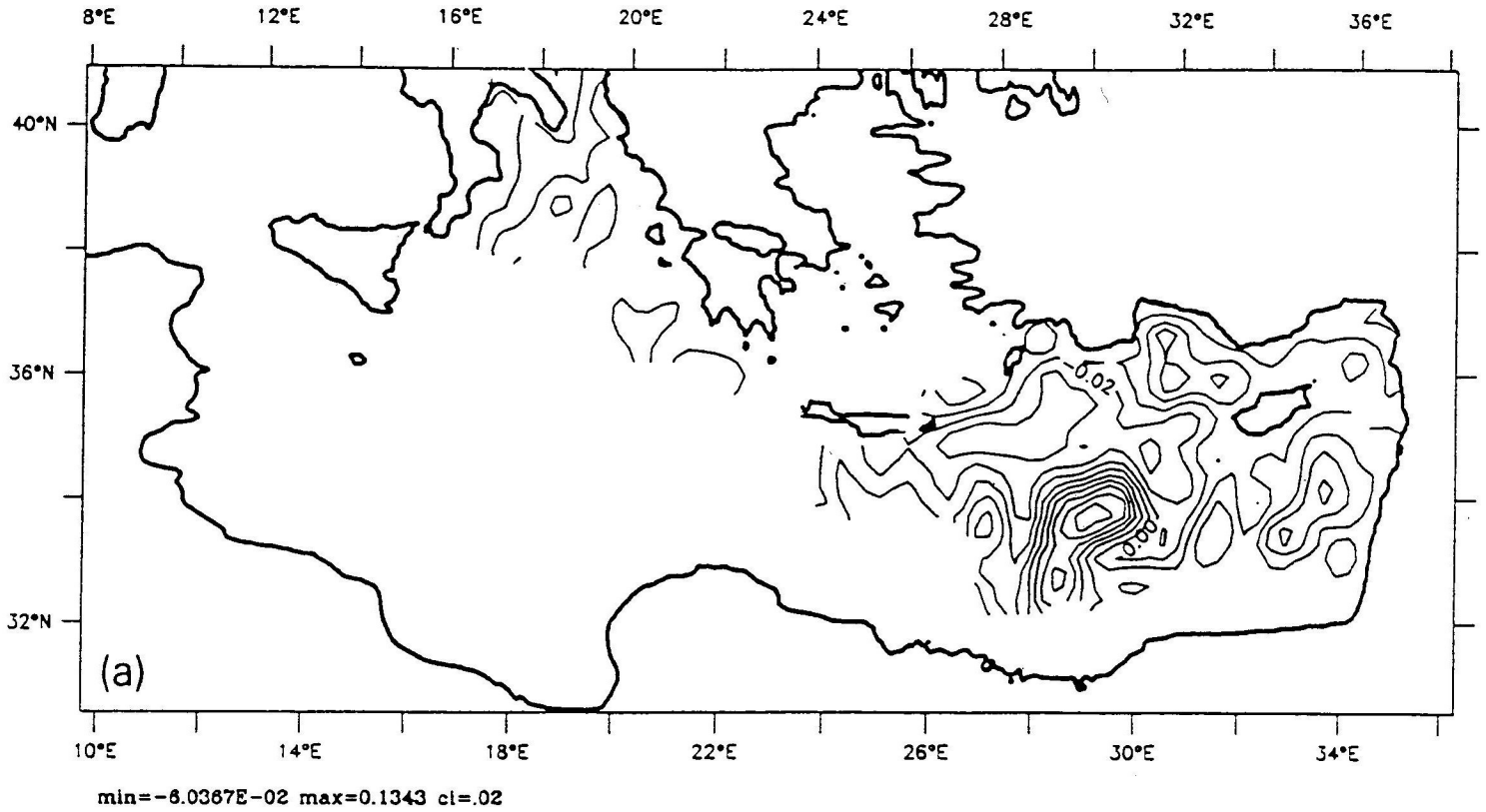

Fig. 9. As in Fig. 7 but for MA 86.

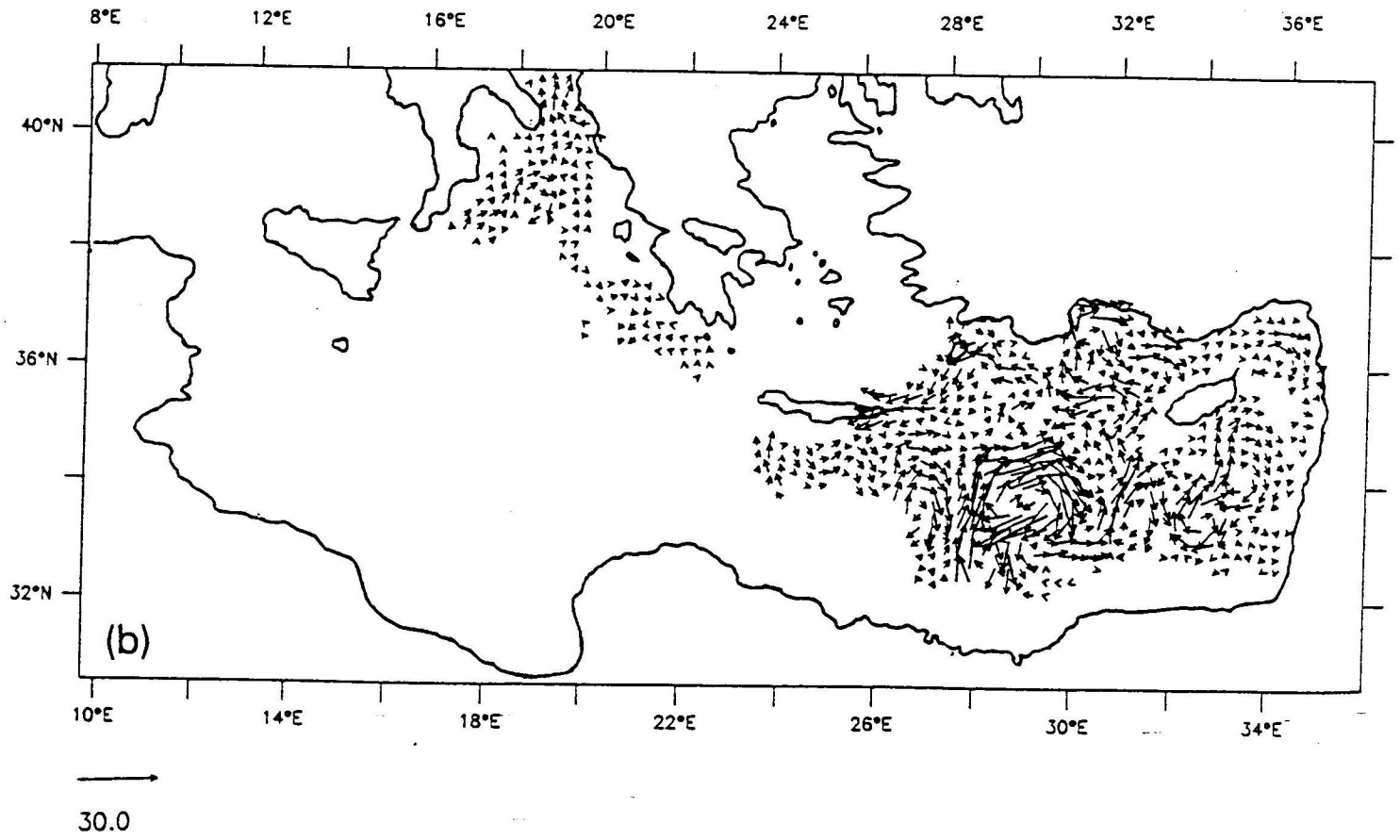

Fig. 9 (continued).

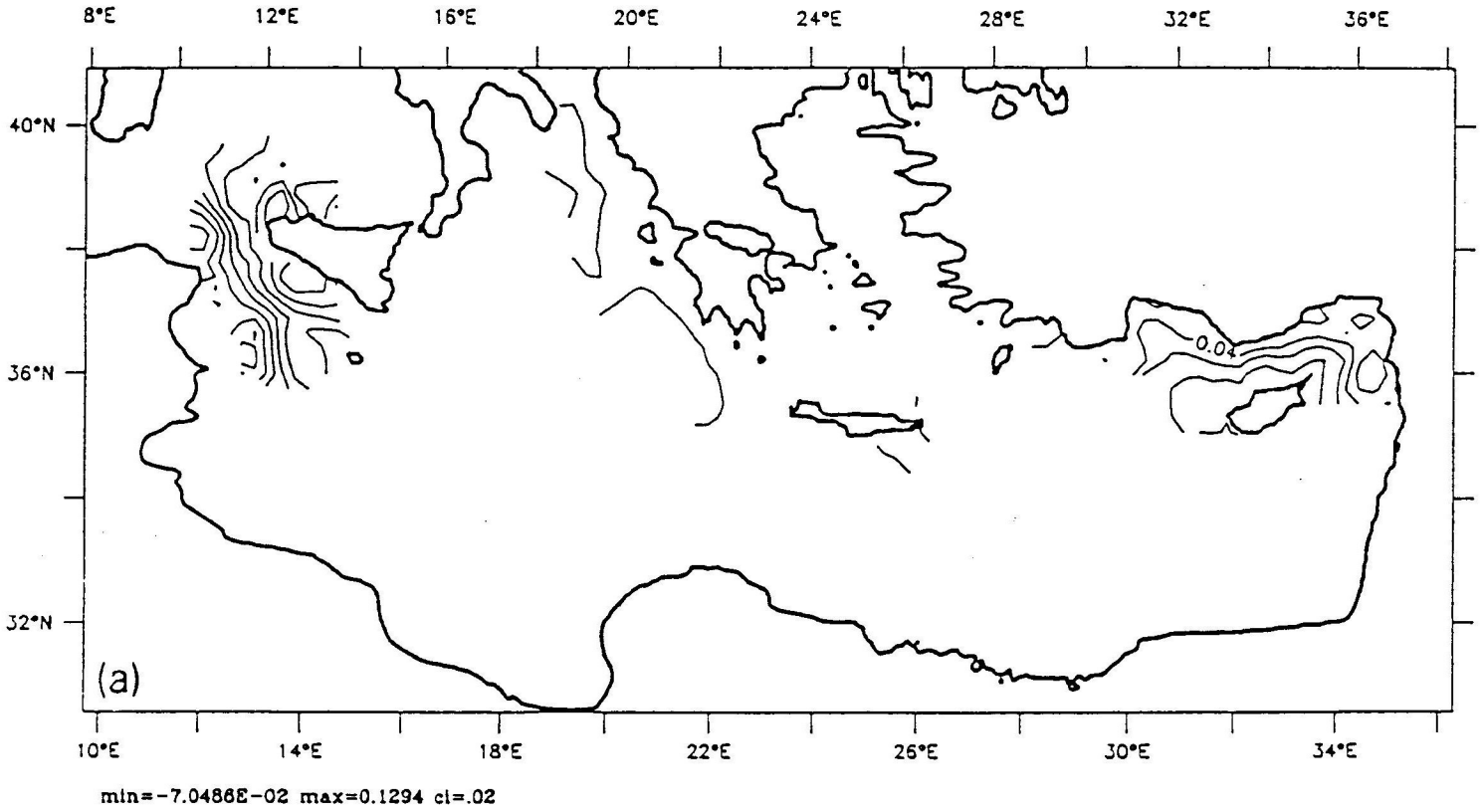

Fig. 10. As in Fig. 7 but for MA 87.

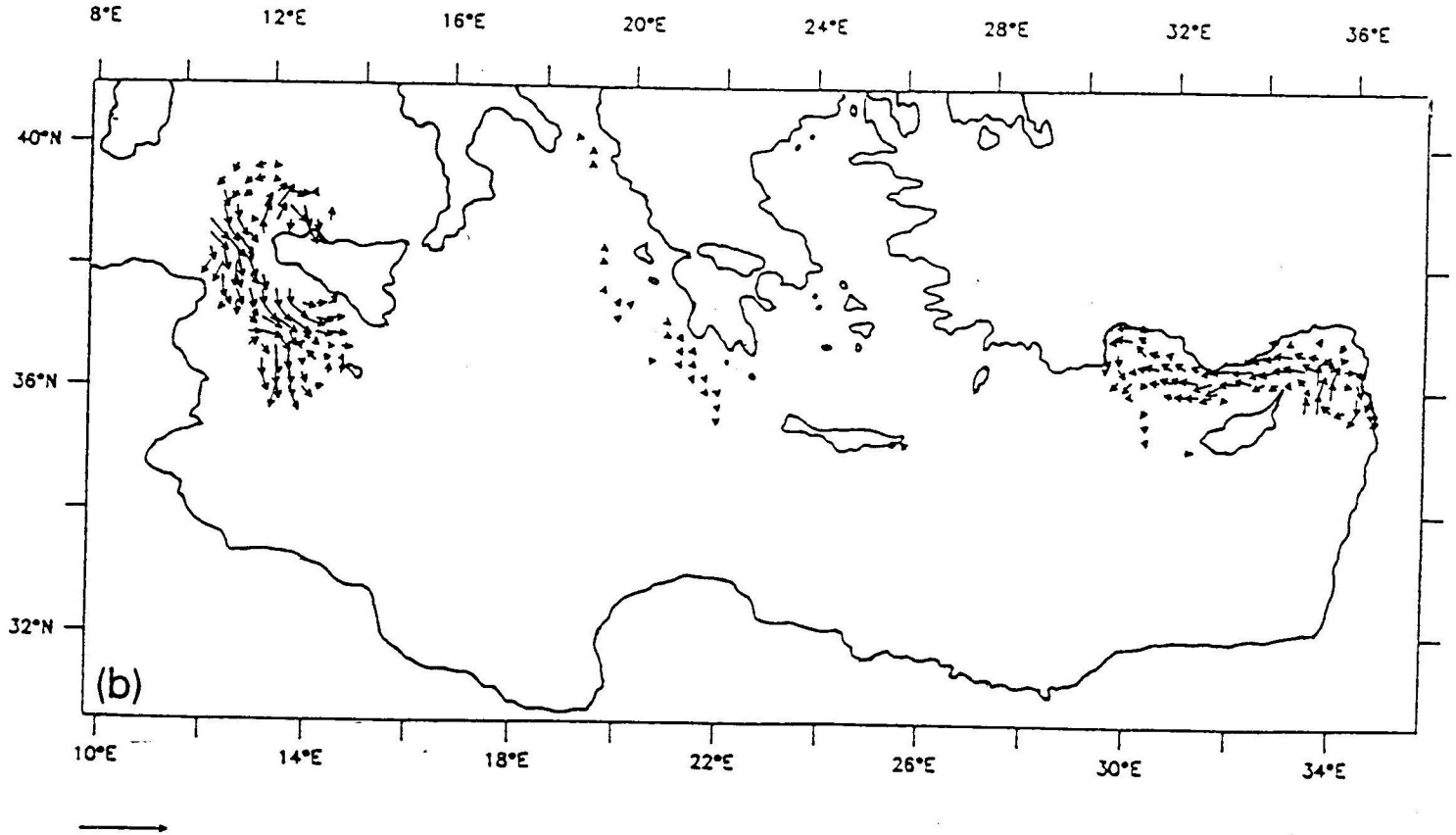

Fig. 10 (continued).

TABLE 3

Upper thermocline features

Features	Type	ON 85	MA 86	MA 87	AS 87
Ionian Atlantic Stream	P	–	–	Y	Y
Mid Med. current	P	Y	Y	–	Y
Asia Minor current	P	Y	Y	–	Y
Cilician current	R	Y	N	Y	N
Southeast Levantine jets	T	Y	Y	–	Y
Rhodes C	P	Y	Y	–	Y
West Cyprus C	P	Y	Y	–	Y
Merse Matruh AC	P	Y	Y	–	Y
Cretan Sea C	P	Y	?	–	Y
Shikmona AC	R	Y	Y	–	Y
Latakia C	R	Y	N	N	Y
Antalya AC	R	?	Y	–	N
Pelops AC	?	–	Y	?	Y
Ionian eddies AC	T	–	–	–	Y
SE Levantine eddies AC	T	Y	Y	–	Y
Cretan Sea eddies	T	Y	Y	–	Y

Definitions: P, Permanent; R, recurrent; T, transient; ?, not enough information to classify; C, cyclone; AC, anticyclone.

southeast Levantine involving the Shikmona eddy and a transient anticyclone. The Mersa–Matruh gyre is flattened and elongated longitudinally in the upper level map. In MA 86 (Fig. 9a, b) the Mersa–Matruh is strong, distorted, and double-centred. The mid-Mediterranean current enters the mapped region flowing northward on the western edge of the Mersa–Matruh. Whether the feature to the west is an intense meander of the current or an eddy is not certain. The southeast Levantine anticyclonic system is still present. The Asia Minor current is relatively weak and shifted southward. The southern edge of the Rhodes gyre has been squeezed northward, a relatively strong Antalya anticyclone exists, and the Pelops anticyclone is present. The Cilician current again appears on MA 87 upper maps (Fig. 10a, b) which also depict the meandering entrance of the Ionian Atlantic stream and hints at the Pelops eddy.

4. CONCLUSIONS

Objectively analysed maps for the relative geostrophic flow of the upper thermocline have been constructed based upon four intercalibrated pooled data sets (Table 1), obtained from basin-wide coordinated surveys. The maps are constrained consistently with no geostrophic flow from deep sea

into coasts. The picture of the general circulation provided by these well-resolved and nearly synoptic realizations of the flow is new. The general circulation consists of permanent and recurrent sub-basin-scale gyres, interconnected by variable currents, and coexisting with transient eddies and interleaving jet segments. A synthesis and summary of the features and structure of the circulation and their variabilities is provided by Fig. 2 and Table 3. Some classifications are preliminary and further observations are required to distinguish, e.g. seasonal from interannual and internal variabilities.

Previous pictures of the general circulation were based classically on water properties (Lacombe and Tchernia, 1972) or on geostrophic calculations from selected data (Ovchinnikov, 1966) or pooled historical data (Anati, 1977, also reviewed in Malanotte-Rizzoli and Hecht, 1988). Lacombe and Tchernia's (1972) classical picture of the summer circulation consists of a broad inflow through the Straits of Sicily, which flows through the southern Ionian bounded on the north by a large cyclone and then fills the Sea of Crete and the western Levantine and flows predominantly cyclonically around the Levantine Basin and Cyprus. Ovchinnikov (1966) distinguishes between summer and winter not by flow structure but only by a stronger winter flow. His circulation pattern consists of an inflow which broadens into the Ionian and is bounded by a northern Ionian cyclone. There is also a cyclonic rim flow around the Levantine Basin and Cyprus. Additional features include a large cyclonic gyre in the Sea of Crete and eastern Ionian and a Rhodes gyre and indications of a meandering Asia Minor current and possibly a weak Mersa–Matruh. Other sub-basin-scale features are questionable. Anati's flow is more complex and structured, especially in summer. The Rhodes gyre is always present and the existence and bifurcation of the mid-Mediterranean jet may be inferred. Other complex features appear to be less credible due to aliasing and historical data pooling. Thus none of these studies have the data resolution or synopticity to reveal the actual circulation constructed from its sub-basin-scale elements as revealed in the present data set. However, some of the broad and general flow characteristics are correctly indicated, while other features are apparently incorrect or missing.

The descriptive and kinematic results presented here provide the basis for extensive dynamic studies and transport estimates. Factors possibly responsible for the sub-basin-scale character of the eastern Mediterranean general circulation include: the dominance of topographic vortex stretching over the planetary beta effect in the presence of variable slopes, topographic interactions, coastlines, multiple and variable forcing functions, and internal dynamic processes. The synthesized and analysed data provide an opportunity not only for dynamic process studies, but also for the initialization, valida-

tion of general circulation models, and assimilation into such models. The data thus assimilated will provide the best estimates of associated transport of interest and importance for interdisciplinary studies and applications.

ACKNOWLEDGEMENTS

We acknowledge, with thanks, the many POEM scientists and technicians whose contributions have made this study possible. We profited from discussions on the circulation with several colleagues, especially Prof. Emin Ozsoy. We thank Prof. Nick P. Fofonoff for useful discussions on data treatment, and a reviewer for helpful comments. This research was supported by NSF Grant OCE-85-8487 and ONR Grant N00014-90-J-1593 to Harvard University.

REFERENCES

Anati, D.A. 1977. Topics in the Physics of Mediterranean Seas, Ph.D. Thesis. Weizmann Institute of Science, Rehovot, Israel, 43 pp.

Carter, E.F. and Robinson, A.R. 1987. Analysis models for the estimation of oceanic fields. J. Atmos. Oceanic Tech., 4: 49–74.

Fofonoff, N.P. and Millard, Jr. R.C. 1983. Algorithms for computation of fundamental properties of sea water. UNESCO Technical Paper in Marine Science, No. 44.

Gregg, M.C., 1979. The effects of bias error and system noise on parameters computed from C, T, P and V profiles. J. Phys. Oceanogr., 9: 199–217.

Hecht, A., Pinardi, N. and Robinson, A.R. 1988. Currents, water masses, eddies and jets in the Mediterranean Levantine Basin. J. Phys. Oceanogr., 18: 1320–1353.

Lacombe, H. and Tchernia, P. 1972. In: D.J. Stanley (Editor), The Mediterranean Sea: A Natural Sedimentation Laboratory. Dowden, Huchinson and Ross, Stroudsburg, PA, pp. 25–36.

Malanotte-Rizzoli, P. and Hecht, A. 1988. Large-scale properties of the eastern Mediterranean: A review. Oceanologica Acta, 11: 323–335.

Malanotte-Rizzoli, P. and Robinson, A.R. 1988. POEM: Physical oceanography of the eastern Mediterranean. EOS, The Oceanography Report, 69: 194–203.

Michelato, A. 1985. Report of the POEM Workshop on Common Procedures for Data Acquisition, Treatment and Intercalibration. OGS (Trieste) Rel/85-115.

Milliff, R.F. 1989. Quasigeostrophic ocean flows in the coastal domains. Harvard Open Ocean Model Reports, 34, Reports in Meteorology and Oceanography, Cambridge, MA. (Ph.D. Thesis, carried out at Harvard for University of California, Santa Barbara.)

Ovchinnikov, I.M. 1966. Circulation in the surface and intermediate layers of the Mediterranean. Oceanology, 24: 168–173.

Özsoy, E., Hecht, A. and Ünlüata, Ü. 1989a. Circulation and hydrology of the Levantine Basin. Results of POEM Coordinated Experiments 1985–1986. Prog. Oceanography, 22: 125–170.

Özsoy, E., Theocharis, A. and Nittis, K. 1989b. POEM Activity Report. Harvard University, Cambridge, MA.

Pinardi, N. 1988. Report of the POEM mapping group: August/September 1987. General Circulation Survey Data Set Preparation, Technical Report No. 1–88.